

Nucleon spin structure at low momentum transfers

Roman S. Pasechnik*

*High Energy Physics, Department of Physics and Astronomy,
Uppsala University Box 516, SE-75120 Uppsala, Sweden*

Jacques Soffer†

*Physics Department, Temple University
Barton Hall, 1900 N, 13th Street
Philadelphia, PA 19122-6082, USA*

Oleg V. Teryaev‡

Bogoliubov Laboratory of Theoretical Physics, JINR, Dubna 141980, Russia

(Dated: May 28, 2022)

Abstract

The generalized Gerasimov-Drell-Hearn (GDH) sum rule is known to be very sensitive to QCD radiative and power corrections. We improve the previously developed QCD-inspired model for the Q^2 -dependence of the GDH sum rule. We take into account higher order radiative and higher twist power corrections extracted from precise Jefferson Lab data on the lowest moment of the spin-dependent proton structure function $\Gamma_1^p(Q^2)$ and on the Bjorken sum rule $\Gamma_1^{p-n}(Q^2)$. By using the singularity-free analytic perturbation theory we demonstrate that the matching point between chiral-like positive- Q^2 expansion and QCD operator product $1/Q^2$ -expansion for the nucleon spin sum rules can be shifted down to rather low $Q \simeq \Lambda_{QCD}$ leading to a good description of recent proton, neutron, deuteron and Bjorken sum rule data at all accessible Q^2 .

PACS numbers: 11.10.Hi, 11.55.Hx, 11.55.Fv, 12.38.Bx, 12.38.Cy

*Electronic address: roman.pasechnik@fysast.uu.se

†Electronic address: jacques.soffer@gmail.com

‡Electronic address: teryaev@theor.jinr.ru

I. INTRODUCTION

The problem of the nucleon spin structure and the peculiarities of its underlying QCD description has attracted a lot of attention over the recent years [1, 2]. In particular, this is due to an enormous progress in experimental studies of the spin sum rules at low momentum transfer Q^2 , from the very accurate Jefferson Lab data on the lowest moment of the spin-dependent proton structure function $\Gamma_1^p(Q^2)$ and on the Bjorken sum rule $\Gamma_1^{p-n}(Q^2)$ in the range $0.05 < Q^2 < 3 \text{ GeV}^2$ [3]. This data provided a good testing ground for combining both the perturbative and non-perturbative QCD contributions.

Theoretical description of the nucleon spin structure functions $g^{p,n}$ at large Q^2 relies on the Operator Product Expansion, and at moderate Q^2 their sensitivity to the radiative and higher twist power corrections becomes significant [4]. Due to such a sensitivity the transition to the entirely non-perturbative Q^2 region is rather cumbersome. This transition was earlier addressed in the QCD-motivated model [5] for the Q^2 -dependence of the generalized Gerasimov-Drell-Hearn (GDH) sum rule [6] making use of the relation to the Burkhardt-Cottingham sum rule [7] for the structure function g_2 , whose elastic contribution is the main source of a strong Q^2 -dependence, while the contribution of the transverse structure function, $g_T = g_1 + g_2$, is smooth. The successful prediction of this model was the distinct “crossover” point of the proton data for $\Gamma_1^p(Q^2)$ at low $Q^2 \sim 200 - 250 \text{ MeV}^2$. Its subsequent modification [8], including radiative and power QCD corrections, made the description far more accurate, which was required by the increased accuracy of the data.

Now we enter a new level of increasing experimental accuracy, obtained in the recently published proton JLab data [3]. They lie above the model inputs at $Q^2 \gtrsim 1.5 \text{ GeV}^2$ (while displaying quite a similar shape) due to a noticeable sensitivity of pQCD part of $\Gamma^{p,n}(Q^2)$ and to poorly known higher twist contributions $\mu_{4,6,\dots}$, as well as the axial singlet charge a_0 .

Our present goal is to improve the model for the generalized GDH sum rule for proton and neutron using the values of the power corrections $\mu_{4,6,\dots}$ and singlet axial charge a_0 , systematically extracted from the JLab data [9, 10] and by performing a similar program of the smooth interpolation between large Q^2 and $Q^2 = 0$. As we will see we are able to achieve a rather good description of the data at all Q^2 values.

The JLab data were obtained in the low Q^2 region and, therefore, a special attention is needed to the QCD coupling in this domain. While the $1/Q^2$ term in the OPE works at relatively high scales $Q^2 \gtrsim 1 \text{ GeV}^2$, higher-twist (HT) power corrections $1/Q^4$, $1/Q^6$, etc., start to play a significant role at lower scales, where the influence of the ghost singularities in the coefficient functions within the standard perturbation theory (PT) becomes more noticeable. It affects the results of extraction of the higher twists from the precise experimental data leading to unstable OPE series and huge error bars [9]. It seems natural that the weakening or elimination of the unphysical singularities of the QCD coupling would allow shifting the perturbative QCD (pQCD) frontier to a lower energy scale and to get more exact information about the nonperturbative part of the process described by the higher-twist series [10].

In this investigation, in order to avoid the influence of unphysical singularities at $Q = \Lambda_{QCD} \sim 400 \text{ MeV}$, we deal with the ghost-free analytic perturbation theory (APT) [11] (for a review on APT concepts and algorithms, see also Ref. [12]), which was recently proven to be an intriguing candidate for a quantitative description of light quarkonia spectra within the Bethe-Salpeter approach [13], as well as in the recent higher-twist analysis of the deep inelastic scattering data on the F_2 structure function [14]. For completeness, we compare our

results obtained with conventional PT and APT couplings and, finally, discuss the related uncertainties and stability issues.

II. FORMALISM

A. OPE regime $Q^2 > \Lambda_{QCD}^2$

To recall the basic ideas of the approach let us consider the lowest moments of spin-dependent proton and neutron structure functions $g_1^{p,n}$ defined as

$$\Gamma_1^{p,n}(Q^2) = \int_0^1 dx g_1^{p,n}(x, Q^2), \quad (2.1)$$

From now on, it is understood that the elastic contribution at $x = 1$ is excluded from the moments, since it is the “inelastic” contribution which can be matched with GDH sum rule.

At large Q^2 the moments $\Gamma_1^{p,n}(Q^2)$ are given by the OPE series in powers of $1/Q^2$ with the expansion coefficients (see, e.g., Ref. [15]). In the limit $Q^2 \gg M^2$ the moments are dominated by the leading twist contribution, $\mu_2^{p,n}(Q^2)$, which can be decomposed into flavor singlet and nonsinglet contributions:

$$\Gamma_1^{p,n}(Q^2) = \frac{1}{12} \left[\left(\pm a_3 + \frac{1}{3} a_8 \right) E_{NS}(Q^2) + \frac{4}{3} a_0 E_S(Q^2) \right] + \sum_{i=2}^{\infty} \frac{\mu_{2i}^{p,n}(Q^2)}{Q^{2i-2}}, \quad (2.2)$$

where E_S and E_{NS} are the singlet and nonsinglet Wilson coefficients, respectively, calculated as series in powers of α_s [16]. These coefficient functions for $n_f = 3$ active flavors in the $\overline{\text{MS}}$ scheme are

$$E_{NS}(Q^2) = 1 - \frac{\alpha_s}{\pi} - 3.558 \left(\frac{\alpha_s}{\pi} \right)^2 - 20.215 \left(\frac{\alpha_s}{\pi} \right)^3 - O(\alpha_s^4), \quad (2.3)$$

$$E_S(Q^2) = 1 - \frac{\alpha_s}{\pi} - 1.096 \left(\frac{\alpha_s}{\pi} \right)^2 - O(\alpha_s^3). \quad (2.4)$$

The triplet and octet axial charges $a_3 \equiv g_A = 1.267 \pm 0.004$ [17] and $a_8 = 0.585 \pm 0.025$ [18], respectively, are extracted from weak decay matrix elements. As for the singlet axial charge a_0 , it is convenient to work with its renormalization group (RG) invariant definition in the $\overline{\text{MS}}$ scheme $a_0 = a_0(Q^2 = \infty)$, in which all the Q^2 dependence is factorized into the definition of the Wilson coefficient $E_S(Q^2)$. For detailed discussion of the higher-loop stability of the coefficient functions and prescriptions used in actual calculations, see Ref. [10].

We address both proton and neutron spin sum rules (SSRs), and the singlet and octet contributions are canceled out in their difference $\Gamma_1^p - \Gamma_1^n$ resulting in the Bjorken sum rule [19]

$$\Gamma_1^{p-n}(Q^2) = \frac{g_A}{6} E_{NS}(Q^2) + \sum_{i=2}^{\infty} \frac{\mu_{2i}^{p-n}(Q^2)}{Q^{2i-2}}. \quad (2.5)$$

The unphysical singularities at $Q \sim \Lambda_{QCD}$ in the PT series for the coefficient functions $E_S(Q^2)$ (2.4) and $E_{NS}(Q^2)$ (2.3) strongly affect the analysis of the spin sum rules at low Q^2 [10]. Their influence becomes essential at $Q < 1$ GeV where the HT terms start to play

an important role. The “soft-frozen” α_s models are free of such a problem, thus providing a more reliable tool of investigating the behavior of the spin sum rules in the low-energy domain.

The moments of the structure functions are analytic functions in the complex Q^2 plane with a cut along the negative real axis, as demonstrated in Refs. [20, 21]. On the other hand, the standard PT approach does not support these analytic properties. The APT method [11] gives the possibility of combining the RG resummation with correct analytic properties of the QCD corrections. The consequence of requiring these properties to hold in the DIS description was studied previously in Refs. [22, 23].

Let us recall that the expression for $\Gamma_1^{p,n}(Q^2)$ in the framework of the analytic approach is completely similar to the one in the standard PT (2.2):

$$\Gamma_{1,APT}^{p,n}(Q^2) = \frac{1}{12} \left[\left(\pm a_3 + \frac{1}{3} a_8 \right) E_{NS}^{APT}(Q^2) + \frac{4}{3} a_0^{inv} E_S^{APT}(Q^2) \right] + \sum_{i=2}^{\infty} \frac{\mu_{2i;p,n}^{APT}(Q^2)}{Q^{2i-2}}. \quad (2.6)$$

The corresponding NNLO APT modification of the singlet and nonsinglet coefficient functions is

$$\begin{aligned} E_{NS}^{APT}(Q^2) &= 1 - 0.318 \mathcal{A}_1^{(3)}(Q^2) - 0.361 \mathcal{A}_2^{(3)}(Q^2) - \dots, \\ E_S^{APT}(Q^2) &= 1 - 0.318 \mathcal{A}_1^{(3)}(Q^2) - 0.111 \mathcal{A}_2^{(3)}(Q^2) - \dots, \end{aligned} \quad (2.7)$$

where $\mathcal{A}_k^{(3)}$ is the analyticized k -th power of three-loop PT coupling in the Euclidean domain and defined as

$$\mathcal{A}_k^{(n)}(Q^2) = \frac{1}{\pi} \int_0^{+\infty} \frac{\text{Im}([\alpha_s^{(n)}(-\sigma, n_f)]^k) d\sigma}{\sigma + Q^2}, \quad n = 3. \quad (2.8)$$

In the one-loop case, the APT Euclidean functions are simple enough [11]:

$$\begin{aligned} \mathcal{A}_1^{(1)}(Q^2) &= \frac{1}{\beta_0} \left[\frac{1}{L} + \frac{\Lambda^2}{\Lambda^2 - Q^2} \right], \quad L = \ln \left(\frac{Q^2}{\Lambda^2} \right), \\ \mathcal{A}_2^{(1)}(l) &= \frac{1}{\beta_0^2} \left[\frac{1}{L^2} - \frac{Q^2 \Lambda^2}{(Q^2 - \Lambda^2)^2} \right], \quad \mathcal{A}_{k+1}^{(1)} = -\frac{1}{k \beta_0} \frac{d\mathcal{A}_k^{(1)}}{dL}. \end{aligned} \quad (2.9)$$

Analogous two- and three-loop level expressions are more involved. However, according to the “effective log” approach [24] in the region $Q < 5$ GeV one may use simple one-loop expressions (2.9) with the *effective logarithm* L^* :

$$\mathcal{A}_{1,2,3}^{(3)}(L) \rightarrow \mathcal{A}_{1,2,3}^{mod} = \mathcal{A}_{1,2,3}^{(1)}(L^*), \quad L^* \simeq 2 \ln(Q/\Lambda_{\text{eff}}^{(1)}), \quad \Lambda_{\text{eff}}^{(1)} \simeq 0.50 \Lambda^{(3)}. \quad (2.10)$$

Thus, instead of the exact three-loop expressions for the APT functions, in Eq. (2.7) one can use the one-loop expressions (2.9) with the effective Λ parameter $\Lambda_{mod} = \Lambda_{\text{eff}}^{(1)}$ whose value is given by the last relation (2.10). This model was successfully applied for higher-twist analysis of low-energy JLab data in Refs. [9, 10], and also in the Υ decay analysis in Ref. [25]. Note also that the APT couplings are stable with respect to different loop orders at low-energy scales $Q^2 \lesssim 1 \text{ GeV}^2$ [12], contrary to the standard PT approach.

The APT functions \mathcal{A}_k contain the $(Q^2)^{-k}$ power contributions, which effectively change the values of the μ -terms, when going from the PT to the APT framework. In particular, by subtracting an extra $(Q^2)^{-1}$ term induced by the APT series for the Bjorken sum rule

$$\Gamma_{1,APT}^{p-n}(Q^2) \simeq \frac{g_A}{6} + f \left(\frac{1}{\ln(Q^2/\Lambda_{\text{eff}}^{(1)2})} \right) + \varkappa \frac{\Lambda_{\text{eff}}^{(1)2}}{Q^2} + \mathcal{O} \left(\frac{1}{Q^4} \right)$$

where $\varkappa \simeq 0.43$ and $\Lambda_{\text{eff}}^{(1)} \sim 0.18$ GeV is the effective one-loop Λ_{QCD} parameter, we get the relation between $\mu_{4,APT}^{p-n}$ coming into the APT expression (2.6) and the conventional μ_4^{p-n} from Eq. (2.2):

$$\frac{\mu_4^{p-n}(1 \text{ GeV}^2)}{M^2} \simeq \frac{\mu_{4,APT}^{p-n} + \varkappa \Lambda_{\text{eff}}^{(1)2}}{M^2}. \quad (2.11)$$

Along with the conventional PT scheme, we will also apply the APT approach based on Eqs. (2.6) and (2.7) to construct the improved model for smooth continuation of perturbative expressions for $\Gamma_1^{p,n}(Q^2)$ and its non-singlet combination $\Gamma_1^{p-n}(Q^2)$ down to the non-perturbative region $Q^2 \rightarrow 0$.

B. “Chiral” regime $Q^2 \lesssim \Lambda_{QCD}^2$

For the purpose of a smooth continuation of $\Gamma_1^{p,n}(Q^2)$ to the non-perturbative region $0 \leq Q^2 \lesssim \Lambda_{QCD}^2$ [5], we consider firstly the Q^2 -evolution of the integral

$$I_1(Q^2) \equiv \frac{2M^2}{Q^2} \Gamma_1(Q^2) = \frac{2M^2}{Q^2} \int_0^1 dx g_1(x, Q^2), \quad (2.12)$$

which is equivalent to the integral over all energies of the spin-dependent photon-nucleon cross-section, whose value at $Q^2 = 0$ is defined by the GDH sum rule [6]

$$I_1(0) = -\frac{\mu_A^2}{4}, \quad (2.13)$$

where μ_A is the nucleon anomalous magnetic moment. Then, the function $I_1(Q^2)$ can be written as a difference

$$I_1(Q^2) = I_T(Q^2) - I_2(Q^2), \quad (2.14)$$

where

$$I_T(Q^2) = \frac{2M^2}{Q^2} \int_0^1 dx g_T(x, Q^2), \quad I_2(Q^2) = \frac{2M^2}{Q^2} \int_0^1 dx g_2(x, Q^2). \quad (2.15)$$

The well-known Burkhardt-Cottingham (BC) sum rule [7] provides us with an exact expression for $I_2(Q^2)$, in terms of familiar electric G_E and magnetic G_M Sachs form factors as

$$I_2(Q^2) = \frac{1}{4} \mu G_M(Q^2) \frac{\mu G_M(Q^2) - G_E(Q^2)}{1 + Q^2/4M^2}, \quad (2.16)$$

where μ is the nucleon magnetic moment. As a consequence of the strong Q^2 behavior of the r.h.s. of Eq. (2.16), we get for large Q^2

$$\int_0^1 g_2(x, Q^2) dx \Big|_{Q^2 \rightarrow \infty} = 0, \quad (2.17)$$

so I_2 is much smaller than I_1 for large Q^2 . Now from the BC sum rule (2.16), it follows that

$$I_2(0) = \frac{\mu_A^2 + \mu_A e}{4} \quad (2.18)$$

where e is the nucleon charge. Then the GDH value (2.13) is reproduced with

$$I_T(0) = \frac{\mu_A e}{4}. \quad (2.19)$$

To summarize, from the above equalities (2.16), (2.17) and (2.19), we can conclude that the BC and GDH sum rules together, lead to positivity of $I_T(Q^2)$ for all Q^2 in the proton case and a vanishing difference between $I_T(Q^2)$ and $I_1(Q^2)$ for large Q^2 . Thus, $I_T^p(Q^2)$ is a smooth and monotonous function, and it is possible to obtain its smooth interpolation between large Q^2 and $Q^2 = 0$ [5].

III. IMPROVED MODEL FOR SMOOTH INTERPOLATION OF $I_T(Q^2)$

To improve the agreement between the model predictions and the experimental data, we consider the general asymptotic expression

$$I_{1,pert}^{p,n}(Q^2) = \frac{2M^2}{Q^2} \left[\frac{1}{12} \left(\pm a_3 + \frac{1}{3} a_8 \right) E_{NS}(Q^2) + \frac{1}{9} a_0 E_S(Q^2) + \sum_{i=2}^{\infty} \frac{\mu_{2i}^{p,n}(Q^2)}{Q^{2i-2}} \right], \quad (3.1)$$

where the nonsinglet E_{NS} and singlet E_S coefficient functions are defined in Eqs. (2.3) and (2.4), respectively. Then, the perturbative expression for I_T , defined above the matching point Q_0^2 , is

$$I_{T,pert}(Q^2) = \Theta(Q^2 - Q_0^2) [I_{1,pert}(Q^2) + I_2(Q^2)], \quad (3.2)$$

where $I_{1,pert}(Q^2)$ is calculated from Eq. (3.1), while $I_2(Q^2)$ is known from the BC sum rule (2.16). The smooth interpolation to the GDH value at $Q^2 = 0$ (2.19) is difficult and cannot be performed analytically. Following the procedure developed in Ref. [5], we instead make use of the smooth extrapolation of the perturbative expression (3.2), to the nonperturbative domain $Q^2 < Q_0^2$ defining the polynomial in positive powers of Q^2 as

$$I_{T,nonpert}(Q^2) = \Theta(Q_0^2 - Q^2) \sum_{n=0}^N \frac{1}{n!} \frac{\partial^n I_{T,pert}}{\partial (Q^2)^n} \Big|_{Q=Q_0} (Q^2 - Q_0^2)^n, \quad (3.3)$$

where N is the number of derivatives, which is a free parameter of the model, together with the matching point $Q = Q_0$, which have to be chosen to satisfy

$$I_{T,nonpert}(0) = \frac{\mu_A e}{4}. \quad (3.4)$$

In practice, the easiest way to solve the problem is to fix the number of derivatives N and then to vary the Q_0 value until the relation (3.4) is satisfied. It is interesting to note that taking $N = 1$ does not allow for such a solution.

Such a procedure can be considered as a matching of the “twist-like” expansion in negative powers of Q^2 and the “chiral-like” expansion in positive powers of Q^2 [5], which is similar to the matching of the expansions in direct and inverse coupling constants.

Once we have obtained the parameters N and Q_0^2 , then the all- Q^2 expressions for the moments $\Gamma_1^{p,n}$ can be restored from $I_T(Q^2)$ defined by Eqs. (3.1) – (3.3), by using Eqs. (2.12) and (2.14). As we will see below, this can be done within both the standard PT and singularity-free APT in the same way, leading to rather similar curves for Q^2 -evolution, except that in the APT case the matching point Q_0^2 playing a role of the “pQCD frontier” in this interpolation scheme is noticeably shifted down to lower Q^2 scales (see the next Section).

IV. HIGHER-TWIST ANALYSIS

A detailed higher twist analysis of the recent Jefferson Lab data [3] on the lowest moments of the spin-dependent proton and neutron structure functions $\Gamma_1^{p,n}(Q^2)$ and $\Gamma_1^{p-n}(Q^2)$ in the range $0.05 < Q^2 < 3 \text{ GeV}^2$ was performed in Refs. [9, 10]. In particular, including only three terms of the OPE expansion $\mu_{4,6,8}$ in Eq. (2.2), a satisfactory description of the data has been achieved down to $Q^2 \simeq 0.17 \text{ GeV}^2$ in conventional PT and down to $Q^2 \simeq 0.10 \text{ GeV}^2$ in the APT.

The lower Q^2 involved, the higher twist contribution is needed to describe the data. As was shown in Ref. [10], there is some sensitivity of fitted values of μ_4 to the minimal scale Q_{min} variations; namely, it increases in magnitude when one incorporates into the fit the data points at lower energies. This property of the fit was treated as the slow (logarithmic) evolution $\mu_4(Q^2)$ (and $a_0(Q^2)$ in the singlet case) with Q^2 which becomes more noticeable for broader fitting ranges in Q^2 , as discussed above. Indeed, fit results for μ_4 with taking into account the RG evolution with $Q = 1 \text{ GeV}$, as a normalization point become more stable with respect to Q_{min} variations.

However, there is still a problem how to treat the evolution of higher-twist terms $\mu_{6,8,..}(Q^2)$ which again may turn out to be important when one goes to lower Q^2 , since the fit becomes more sensitive to very small variations of $\mu_{6,8,..}$ with Q^2 . Since the evolution of the higher twists $\mu_{6,8}$ is still theoretically unknown, they can be taken as free parameters [26]. This procedure leads to rather small $\chi_{D.o.f}^2 \sim 0.1$ since more free parameters come into a fit at lower Q^2 . On the other hand, by including $\mu_{6,8,..}$ into the fit, one observes only a small change in $\mu_4(1 \text{ GeV}^2)$ [10], which demonstrates its stability down to lower Q^2 . Taking this into account, in order to reduce the number of free parameters, in the current work we apply another fitting procedure and determine, first, μ_4 and a_0 at higher scale $Q = 1 \text{ GeV}$. Then we extract μ_6 applying the known QCD evolution for $\mu_4(Q^2)$ and $a_0(Q^2)$ and fixing them at 1 GeV from the previous fit. The number of free parameters does not grow in this case. The fitting domain is restricted from below by Q_{min} defined by the condition $\chi^2/D.o.f \leq 1$. The corresponding results are listed in Table I. Due to unknown evolution of $\mu_6(Q^2)$, which tends to be quite noticeable at lower Q^2 , we do not go below Q_{min} and do not take into account μ_8 -term here.

The advantage of the APT analysis is the infrared and higher loop stability of the radiative corrections, as well as the stability w.r.t. Λ_{QCD} variations, leading to the stability and convergence of the higher twist series extracted from the data. Indeed, as we see from

Table I, in the APT case the applicability of the perturbative expansion (2.6) is somewhat shifted down to lower Q^2 , due to the absence of Landau singularities (see also Ref. [10] and references therein).

V. ALL- Q^2 SPIN SUM RULES

In the perturbative expression (3.1) we take into account the two-loop perturbative correction in the singlet E_S and non-singlet E_{NS} coefficient functions, as well as the twist-4,6 contributions discussed in the previous section. To explore the infrared sensitivity of the model of the smooth continuation to $Q = 0$, we used two different sets of higher twist terms (with μ_4 and $\mu_{4,6}$, respectively) and the corresponding singlet axial charge extracted from the data above a certain minimal scale Q_{min}^2 .

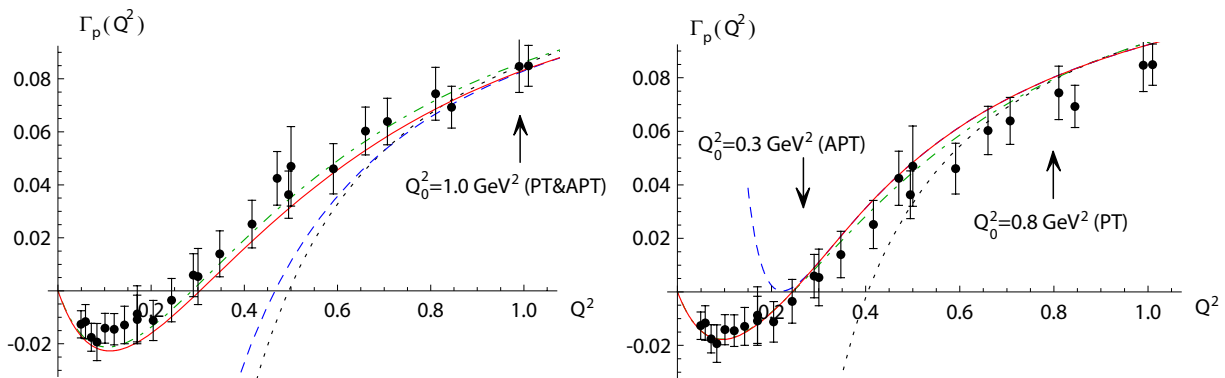


FIG. 1: Proton spin sum rule function $\Gamma_1^p(Q^2)$ with respect to the combined set of JLab and SLAC data. Results are shown with an account of the twist-4 term (left panel) and the twist-4,6 terms (right panel). Corresponding perturbative parts are calculated in the framework of conventional PT (dotted lines) and APT (dashed lines). All- Q^2 model function obtained by the smooth interpolation of $I_T^p(Q^2)$ is also presented in PT (dash-dotted lines) and APT (solid lines).

In Fig. 1 we present the proton spin sum rule function $\Gamma_1^p(Q^2)$ obtained by the smooth interpolation of the perturbative part $I_{T,perp}^p(Q^2)$ to the non-perturbative region $Q^2 \rightarrow 0$ as described in Section III. Calculations taking into account one twist-4 term (left panel) and two twist-4,6 terms (right panel) listed above are performed within the conventional PT and APT. In Fig. 2 we show the Bjorken sum rule function $\Gamma_1^{p-n}(Q^2)$ calculated at any Q^2 in the similar way as $\Gamma_1^p(Q^2)$.

The all- Q^2 model functions $\Gamma_1^p(Q^2)$ and $\Gamma_1^{p-n}(Q^2)$ in both versions of the perturbation theory (dash-dotted and solid lines) are rather close to each other demonstrating the agreement between the singularity-free APT analysis at lower Q^2 and the usual PT one at relatively higher Q^2 . Also, as one can see from the comparison of the left and right panels the results of the interpolation do not strongly depend on the number of higher twists included and, hence, on the border Q_0^2 between perturbative and non-perturbative regimes. This exhibits a sort of duality between them implying that the experimental data in the wide intermediate region $\Lambda_{QCD}^2 \lesssim Q^2 \sim 1 \text{ GeV}^2$ can be described equally well either by OPE $1/Q^2$ -series or by “chiral-like” Q^2 -series.

We studied the sensitivity of above results w.r.t. variations of the number of derivatives N in Eq. (3.3) being the number of positive $\sim Q^{2i}$ power terms. As mentioned above, at

TABLE I: Combined fit results of JLab and SLAC data on the Bjorken SR and proton SSR for the singlet axial charge a_0 , and the higher-twist terms μ_4 and μ_6 defined at the normalization point $Q^2 = 1 \text{ GeV}^2$ in the APT and the standard PT approaches, along with the matching value Q_0^2 . Corresponding curves for $\Gamma_1^p(Q^2)$ and $\Gamma_1^{p-n}(Q^2)$ are shown in Figs. 1 and 2, respectively. Typical values of $\chi^2/D.o.f$ are close to unity.

Method	Target	$Q_{min}^2, \text{ GeV}^2$	a_0	μ_4/M^2	μ_6/M^4	$Q_0^2, \text{ GeV}^2$
NLO PT	p-n	1.0	–	$-0.060(3)$	0	1.1(2)
		0.3	–	-0.060	0.010(2)	0.8(2)
	proton	1.0	0.34(3)	$-0.056(3)$	0	1.0(1)
		0.5	0.34	-0.056	0.010(2)	0.8(2)
NLO APT	p-n	1.0	–	$-0.058(3)$	0	1.0(1)
		0.2	–	-0.058	0.010(1)	0.3(1)
	proton	1.0	0.37(2)	$-0.063(2)$	0	1.0(1)
		0.3	0.37	-0.063	0.011(1)	0.3(1)

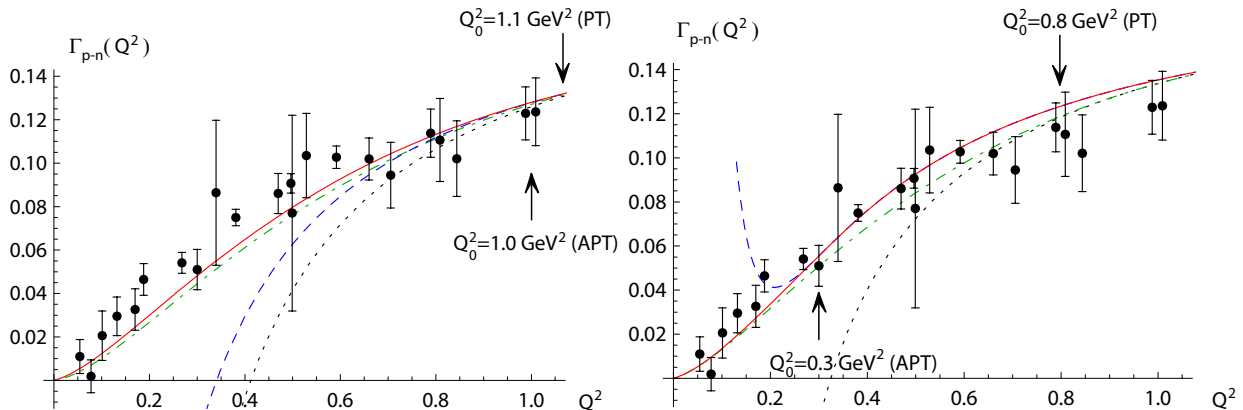


FIG. 2: Bjorken sum rule function $\Gamma_1^{p-n}(Q^2)$ with respect to the combined set of JLab and SLAC data. The meaning of curves here is the same as in Fig. 1.

lower Q^2 we need more higher $1/Q^2$ -power twist terms. In the same way, going up from very low Q^2 we observe analogously that to describe the data at higher Q^2 we need more $\sim Q^{2i}$ power terms, i.e. a higher value N .

The minimal number of derivatives N_{min} , which is necessary to perform the smooth extrapolation according to Eq. (3.3) in the conventional PT case and with one μ_4 term only, is $N_{min} = 4$. Corresponding matching value between perturbative and non-perturbative domains in this case is found to be $Q_0^2 = 1.0 \pm 0.1 \text{ GeV}^2$ for the proton SSR and $Q_0^2 = 1.1 \pm 0.2 \text{ GeV}^2$ for the Bjorken SR (see Table I). However, if one increases the number of Q^2 -power term up to $N = 6$, the applicability of the “chiral-like” expansion raises up to $Q_0^2 \simeq 1.4 \text{ GeV}^2$ for the proton SSR and $Q_0^2 \simeq 1.5 \text{ GeV}^2$ for the Bjorken SR. Similar observation was made earlier in Ref. [5].

In the framework of APT the minimal number of derivatives $N_{min} = 3$ is even smaller than in the conventional PT. In this case, if only one μ_4 term is included then the matching

value turned out to be same as in PT: $Q_0^2 \simeq 1.0 \text{ GeV}^2$ for both the proton SSR and $p - n$ demonstrating the similarity of the APT and PT predictions at $Q \gtrsim 1 \text{ GeV}$.

However, analysis at lower Q^2 including two $\mu_{4,6}$ terms leads to quite different Q_0 values for PT and APT. In this case, for the proton SSR and Bjorken SR we have $Q_0^2 \simeq 0.8 \pm 0.2 \text{ GeV}^2$ (PT, $N_{min} = 3$) and $Q_0^2 \simeq 0.32 \pm 0.1 \text{ GeV}^2$ (APT, $N_{min} = 2$). Such a shift of the border between perturbative and non-perturbative domains in the APT is a direct consequence of the disappearance of the unphysical singularities in the radiative corrections, and confirms the similar conclusion made in Refs. [9, 10].

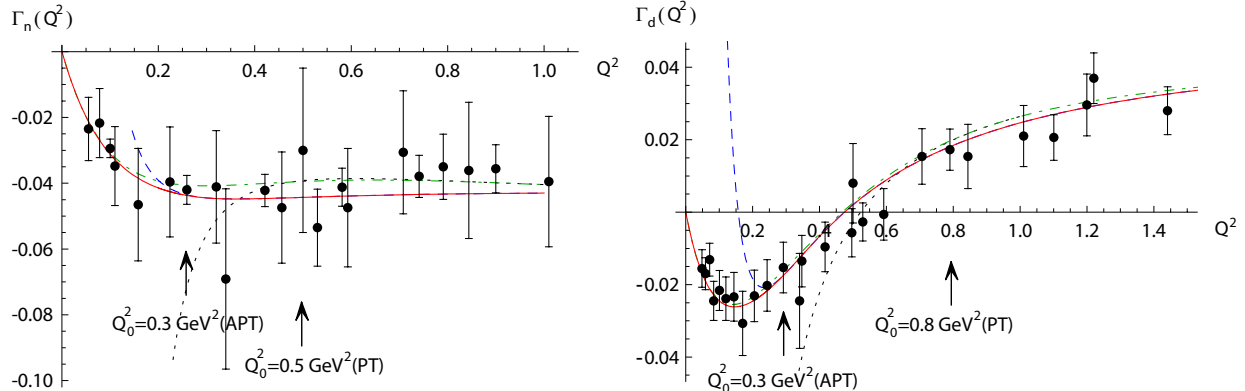


FIG. 3: Neutron (left) and deuteron (right) spin sum rule functions, $\Gamma_1^n(Q^2)$ and $\Gamma_1^d(Q^2)$, with respect to the combined set of JLab and SLAC data. Results are shown with an account of twist-4,6 terms. The meaning of curves here is the same as in Fig. 1.

Finally, in Fig. 3 we show the neutron spin sum rule function $\Gamma_1^n(Q^2)$, which is simply obtained from the difference $\Gamma_1^p(Q^2) - \Gamma_1^{p-n}(Q^2)$, and the deuteron spin sum rule $\Gamma_1^d(Q^2)$. We also present its perturbative PT and APT parts together with less precise data. Both versions of the perturbation theory predict monotonous curves for $\Gamma_1^{n,d}(Q^2)$ at any Q^2 . Comparison between them and the results of Ref. [10] demonstrates the consistence of the direct fits to the data and the predictions of the generalized GDH sum rule.

VI. CONCLUSION

In the current paper we have considered the all- Q^2 model for the generalized GDH sum rule, constructed by the smooth interpolation of $I_T(Q^2)$ between large Q^2 and $Q^2 = 0$, in the framework of both the conventional PT and the ghost-free Analytic Perturbation Theory. We used the values of the power corrections $\mu_{4,6,\dots}$ and singlet axial charge a_0 , systematically extracted from the precise JLab data. We achieve a rather good description of the proton data on $\Gamma_1^p(Q^2)$ at any Q^2 values. We also present an improved description of the neutron data, as well as the Bjorken sum rule data at all experimentally accessed Q^2 .

The results of the smooth interpolation $\Gamma_1^p(Q^2)$ and $\Gamma_1^{p-n}(Q^2)$ do not strongly depend on the number of higher-twist terms, and on the border Q_0^2 between perturbative and non-perturbative regimes. This exhibits a sort of duality between them implying that the experimental data in the wide intermediate region $\Lambda_{QCD}^2 \lesssim Q^2 \sim 1 \text{ GeV}^2$ can be described equally well either by OPE $1/Q^2$ -series or by non-perturbative “chiral-like” Q^2 -series. Within the analytic PT the “pQCD frontier” being the matching value between Q^2 - and $1/Q^2$ -power

series naturally decreases from 1.0 GeV^2 with single μ_4 down to 0.3 GeV^2 with extra μ_6 -term included, which is significantly lower than the corresponding value in conventional PT $Q_0^2 \simeq 0.8 \text{ GeV}^2$. Such a shift of the border between perturbative and non-perturbative domains in the APT is a direct consequence of the disappearance of the unphysical singularities in the radiative corrections.

ACKNOWLEDGMENTS

We are thankful to A.P. Bakulev, J.P. Chen, G. Dodge, S.B. Gerasimov, G. Ingelman, A.L. Kataev, O.V. Selyugin, A.V. Sidorov, D.B. Stamenov, and N.G. Stefanis for valuable discussions. This work was partially supported by the Carl Trygger Foundation and by RFBR Grants No. 09-02-00732, 09-02-01149.

-
- [1] M. Anselmino, A. Efremov and E. Leader, Phys. Rept. **261**, 1 (1995) [Erratum-ibid. **281**, 399 (1997)].
 - [2] S. E. Kuhn, J. P. Chen and E. Leader, Prog. Part. Nucl. Phys. **63**, 1 (2009).
 - [3] K. V. Dharmawardane *et al.*, Phys. Lett. **B 641** 11 (2006);
P. E. Bosted *et al.*, Phys. Rev. C **75**, 035203 (2007);
Y. Prok *et al.* [CLAS Collaboration], Phys. Lett. B **672**, 12 (2009).
 - [4] S. A. Larin, F. V. Tkachov and J. A. Vermaseren, Phys. Rev. Lett. **66**, 862 (1991);
S. A. Larin and J. A. Vermaseren, Phys. Lett. B **259**, 345 (1991);
M. Anselmino, B. L. Ioffe and E. Leader, Sov. J. Nucl. Phys. **49**, 136 (1989);
V. M. Braun and A. V. Kolesnichenko, Nucl. Phys. B **283**, 723 (1987).
 - [5] J. Soffer and O. Teryaev, Phys. Rev. Lett. **70**, 3373 (1993).
 - [6] S. B. Gerasimov, Sov. J. Nucl. Phys. **2**, 430 (1966) [Yad. Fiz. **2**, 598 (1966)];
S. D. Drell and A. C. Hearn, Phys. Rev. Lett. **16**, 908 (1966).
 - [7] H. Burkhardt and W. N. Cottingham, Annals Phys. (N.Y.) **16**, 543 (1970).
 - [8] J. Soffer and O. Teryaev, Phys. Rev. D **70**, 116004 (2004).
 - [9] R. S. Pasechnik, D. V. Shirkov and O. V. Teryaev, Phys. Rev. D **78**, 071902 (2008) [arXiv:0808.0066 [hep-ph]].
 - [10] R. S. Pasechnik, D. V. Shirkov, O. V. Teryaev, O. P. Solovtsova and V. L. Khandramai, Phys. Rev. D **81**, 016010 (2010) [arXiv:0911.3297 [hep-ph]].
 - [11] D. V. Shirkov and I. L. Solovtsov, JINR Rapid Comm. **2** [76-96], 5 (1996) [arXiv:hep-ph/9604363]; Phys. Rev. Lett. **79**, 1209 (1997);
K. A. Milton and I. L. Solovtsov, Phys. Rev. D **55**, 5295 (1997).
 - [12] D. V. Shirkov and I. L. Solovtsov, Theor. Math. Phys. **150**, 132 (2007).
 - [13] M. Baldicchi, A. V. Nesterenko, G. M. Prospero, D. V. Shirkov and C. Simolo, Phys. Rev. Lett. **99**, 242001 (2007).
 - [14] A. V. Kotikov, V. G. Krivokhizhin and B. G. Shaikhatdenov, arXiv:1008.0545 [hep-ph].
 - [15] A. L. Kataev, Phys. Rev. D **50**, 5469 (1994); Mod. Phys. Lett. A **20**, 2007 (2005).
 - [16] S. A. Larin, T. van Ritbergen and J. A. M. Vermaseren, Phys. Lett. B **404**, 153 (1997).
 - [17] C. Amsler *et al.* [Particle Data Group], Phys. Lett. B **667**, 1 (2008).
 - [18] Y. Goto *et al.* [Asymmetry Analysis collaboration], Phys. Rev. D **62**, 034017 (2000).

- [19] J. D. Bjorken, Phys. Rev. **148**, 1467 (1966); Phys. Rev. **D1**, 1376 (1970).
- [20] W. Wetzel, Nucl. Phys. B **139**, 170 (1978).
- [21] Ashok suri, Phys. Rev. D **4**, 570 (1971).
- [22] K. A. Milton, I. L. Solovtsov and O. P. Solovtsova, Phys. Rev. D **60**, 016001 (1999).
- [23] K. A. Milton, I. L. Solovtsov and O. P. Solovtsova, Phys. Lett. B **439**, 421 (1998).
- [24] I. L. Solovtsov and D. V. Shirkov, Theor. Math. Phys. **120**, 1220 (1999).
- [25] D. V. Shirkov and A. V. Zayakin, Phys. Atom. Nucl. **70**: 775-783, (2007).
- [26] A. Deur, arXiv:nucl-ex/0508022.